ORIGINAL PAPER

Fluorescence Quenching of 1,4-Dihydroxy-2, 3-Dimethyl-9,10-Anthraquinone by Silver Nanoparticles: Size Effect

M. Umadevi · P. Vanelle · T. Terme · Beulah J. M. Rajkumar · V. Ramakrishnan

Abstract Size effect of silver nano particles on the photophysical properties of 1,4-dihydroxy-2,3-dimethyl-9,10-anthraquinone (DHDMAQ) have been investigated using optical absorption and fluorescence emission techniques. Silver nanoparticles of different sizes have been prepared by Creighton method using magnetic stirrer and ultrasonic field. Quenching of fluorescence of DHDMAQ has been found to increase with decrease in the size of the silver nanoparticles. Stern–Volmer quenching constants have also been calculated.

M. Umadevi (✉)
Department of Physics, Mother Teresa Women's University,
Kodaikanal 624 102, Tamil Nadu, India
e-mail: ums10@yahoo.com

P. Vanelle · T. Terme
Department of Radical Pharmaco-Chemistry, UMR CNRS 6264,
Faculty of Pharmacy, University of Méditerranée,
27 Bd Jean Moulin,
13385 Marseille Cedex 5, France

B. J. M. Rajkumar
Department of Physics, Lady Doak College,
Madurai, India

V. Ramakrishnan
Department of Laser Studies, School of Physics,
Madurai Kamaraj University,
Madurai 625 021, India

Introduction

Amino and dihydroxy substituted quinones are an important class of molecules, having immense importance in the dye industry, biology and pharmaceutical chemistry [1, 2]. Dihydroxy anthraquinones are compounds of significant chemical and biological interest. These molecules have important applications as a prominent family of pharmaceutically active and biologically relevant chromophores, as an analytical tool for the determination of metals and in many aspects of electrochemistry [3]. The hydroxy anthraquinone chromophore is the biologically active site in several antitumor anthracyclines. The stacking interaction between the chromophore of the drug and the base pairs of DNA has been studied by means of several spectroscopic studies. The preparation of uniform nanosized drug particles with specific requirements in terms of size, shape and physical and chemical properties is of great interest in the formulation of new pharmaceutical products [4, 5]. Hydroxy anthraquinone in certain medicinal plants such as *Rubia tinctorium* L. is a genotoxic and rodent colon carcinogen [6–8]. Hydroxy anthraquinone derivatives have been isolated from the roots of *Prismatomeris tetrandra* and *Rubia cordiofolia* L.[9, 10]. Hydroxy anthraquinone glycosides are concentrated in leaves and flowers of *Cassia fistula* Linn [11]. It is also found in leaves and bark of *Cassia podocarpa*. It enhances its commercialization as a laxative due to its antimicrobial effect [12].

The integration of nanotechnology with biology and medicine is expected to produce major advances in molecular diagnostics, therapeutics and bioengineering [13, 14]. Nanoparticles in the diameter range 1–100 nm would display new physical properties that are neither those of bulk metal nor those of molecular compounds. These properties strongly depend on the particle size, inter particle

distance, nature of the protecting organic shell and shape of the nanoparticles [13]. Nanoscale metal particles have attracted significant attention because of their unusual size dependent optical and electronic properties. These nanomaterials have found potential applications in electronics, nonlinear optics, chemical and biochemical sensors, and in catalysis [15]. Due to surface plasmon excitation, nanoparticles of silver, gold and copper may exhibit sharp electronic absorption bands in the visible region [16]. The size, shape and structure of nanoparticles define their properties. Further the development of new procedures for the synthesis of nanomaterials with a well defined morphology is a very important research target [17]. Assembling fluorophore-metal nanoparticles superstructures as a two or three dimensional architecture provides routes to design novel materials with tailored electrical, optical, lithographic, sensing and photochemical properties [18, 19]. Resonant energy transfer systems consisting of organic dye molecules and noble metal nanoparticles have recently gained considerable interest in biophotonics as well as in materials science [20].

The biological importance of 1,4-dihydroxy-2,3-dimethyl-9,10-anthraquinone (DHDMAQ) molecule and silver nanoparticles has prompted to the study the photo physical properties and the influence of size effect of silver nanoparticles on this molecule. Interaction of a dye with the medium at the molecular level is reflected in its visible and fluorescence spectra [21]. Fluorescence quenching is a technique to understand the interaction within the medium in view of the special role of surfaces of the nanoclusters in guiding and modifying physicochemical processes.

In the present study, optical absorption and fluorescence emission spectroscopic techniques have been employed to investigate the effect of silver nanoparticles on 1,4-dihydroxy-2,3-dimethyl,9,10-anthraquinone (Fig. 1).
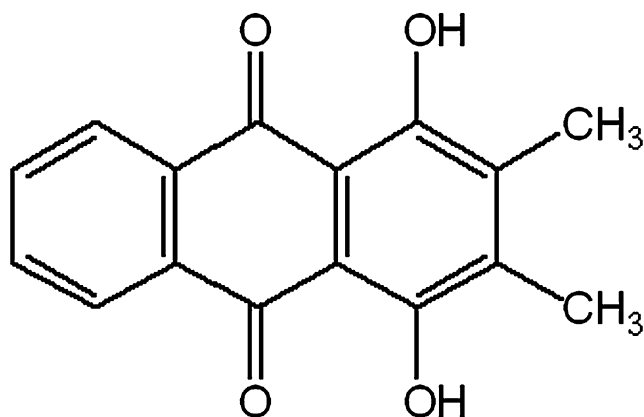

Fig. 1 Structural formula of 1,4-dihydroxy-2,3-dimethyl-9,10-anthraquinone

Experimental

Reagents

Spectral grade methanol was obtained from SISCO laboratory and was used without further purification. Silver nitrate and sodium borohydride, purchased from Aldrich, were used as received. 1,4-Dihydroxy-2,3-dimethyl-9,10-anthraquinone was prepared according to the literature [22]. Doubly distilled water was used throughout.

Procedure

The silver nanoparticles used in this study were synthesized by two different methods.

In the first method silver sol were prepared according to Creighton method [23]. In brief 2 ml of silver nitrate solution (0.6 mM) was added drop wise to 25 ml of sodium borohydride solution (1.2 mM) with vigorous stirring. It was repeated for different volume of sodium borohydride (4, 8 and 10 ml) at constant volume of silver nitrate solution (25 ml). Both the solutions were chilled to ice temperature.

In the second method, in the presence of ultrasonic field (150 KHz), 2 ml of silver nitrate solution (0.6 mM) was added drop wise to 25 ml of sodium borohydride solution (1.2 mM). It was repeated for different volume of silver nitrate solution (4, 8 and 10 ml) at constant volume of sodium borohydride solution (25 ml). The ultrasonic treatment time was 1 h 30 min for all the cases. Both the solutions were chilled to 0 °C.

The concentration of DHDMAQ in methanol was 0.02 mM. For the effect of silver nanoparticles on DHDMAQ, DHDMAQ in methanol and silver sol have been taken in 1:1 volume ratio.

Fluorescence quantum yield

Parker's method was employed to determine the relative fluorescence quantum yield (ϕ_{rel}) [24] in which 2,3-dichloromethyl-1,4-anthraquinone in dichloromethane was used as fluorescence standard ($\phi = 4.87 \times 10^{-3}$) [25]. In the present case the fluorescence quantum yield of DHDMAQ in methanol was found to be 1.0836.

Apparatus

Optical absorption spectra were recorded using a (Shimadzu UV-1700 PharmaSpec) UV–visible spectrophotometer. Elico Spectrofluorometer SL174 was used to record fluorescence spectra. For fluorescence measurements the excitation wavelength was 488 nm.

Results and discussion

Silver nano particle size determination

Gustav Mie was the first to provide an explanation on the dependence of color on the metal particle size [26]. Surface plasmon resonance can be thought of as the collective oscillation of the conduction band electrons in the metals. This is due to the small size of the particle and surface property and is not exhibited by individual atoms or bulk materials. When the size of the particle is less than one tenth of the wavelength of the incident light, the electric fields can be assumed as spatially constant and only the temporal variation is taken into account. This state is called the quasi-static regime. Conduction bands electrons of alkali and noble metals interact strongly with the visible range of the electromagnetic waves. The incoming electric field of the electromagnetic wave induces a polarization of the electron with respect to the heavy ionic nucleus. The net charge difference is felt only at the surface (surface as defined by depth of penetration of the electromagnetic wave), which, it compensates with a restoring force in the form of a dipolar oscillation of the surface electrons in the same phase [27]. However when the size of the particle is comparable to their skin depth, all the electrons in the particle resonates, resulting in strong absorption of the particular wavelength. Since skin depth is dependent on the wavelength of the incident wave, particles of different sizes resonate at different wavelengths. This gives rise to different colors of silver colloid. The color of the colloid depends not just on the particle size, but also on the shape, the refractive index of the surrounding media and the separation between the particles. A change in any of these parameters will result in the quantifiable shift in the surface plasmon resonance absorption peak [28].

The optical properties of dispersions of spherical particles with a radius R can be predicted by Mie theory [26], through expression for the extinction cross section C_{ext}. For very small particles with a frequency dependent, complex dielectric function, $\varepsilon = \varepsilon' + i\varepsilon''$, embedded in a medium of dielectric constant ε_m this can be expressed as

$$C_{ext} = \frac{24\pi^2 R^3 \varepsilon_m^{3/2}}{\lambda} \frac{\varepsilon''}{(\varepsilon' + 2\varepsilon_m)^2 + \varepsilon''^2} \quad (1)$$

The origin of the strong color changes displayed by small particles lies in the denominator of equation which predicts the existence of an absorption peak when

$$\varepsilon' = -2\varepsilon_m \quad (2)$$

In a small metal particle, the dipole created by the electric field of light induces a surface polarization charge which effectively act as a restoring force for the free electrons. The net result is that, when condition Eq. 2 is fulfilled, the long wavelength absorption by the bulk metal is condensed into a small surface plasmon band. Using this Mie theory the radius of the silver nanoparticles have been calculated (Table 1).

In ultrasonic bath, standing wave field is formed in a flat bottomed vessel and a diffusion field is formed in a round bottomed flask. In the present case, silver colloids were prepared in the flat bottomed vessel with standing wave field. It is evident that in standing wave field the silver colloidal particles are spherical, hexagonal or irregular shaped. Apparently, this is associated with the ultrasonic field distribution in the reaction vessel. Specifically, a standing wave is a stack of two same amplitude coherent waves traveling along a straight line but in reverse direction. After stacking, the standing wave only fluctuates in a limited area, but does not propagate outwards. Therefore, in a standing wave field, the particles can grow along some directions into a regular shape from a sphere like or irregular shape [29].

In the present case the absorption spectrum has a maximum in the range 380–400 nm, which is related to the plasmon band of the formed nanosized silver particles (Fig. 2a and b). This absorption band results from interactions of free electrons confined to small metallic

Table 1 Photophysical properties of DHDMAQ in silver nanoparticles

| S. No.	Volume of aqueous (ml) AgNO$_3$:NaBH$_4$	Particle size (radius) (nm)	Quantum yield (ϕ)	Concentration of silver [Ag] (mM)	ΔA at 488 nm
Using magnetic stirrer					
1	2:25	21.5	0.1889	0.0444	0.002
2	4:25	17.0	0.1059	0.0828	0.084
3	8:25	16.0	0.0855	0.1455	0.145
4	10:25	15.0	0.0542	0.1714	0.189
Using ultrasonic field					
1	2:25	19.0	0.1446	0.0444	0.012
2	4:25	13.0	0.0925	0.0828	0.056
3	8:25	6.0	0.0799	0.1455	0.100
4	10:25	<5	0.0431	0.1714	0.218

a

b
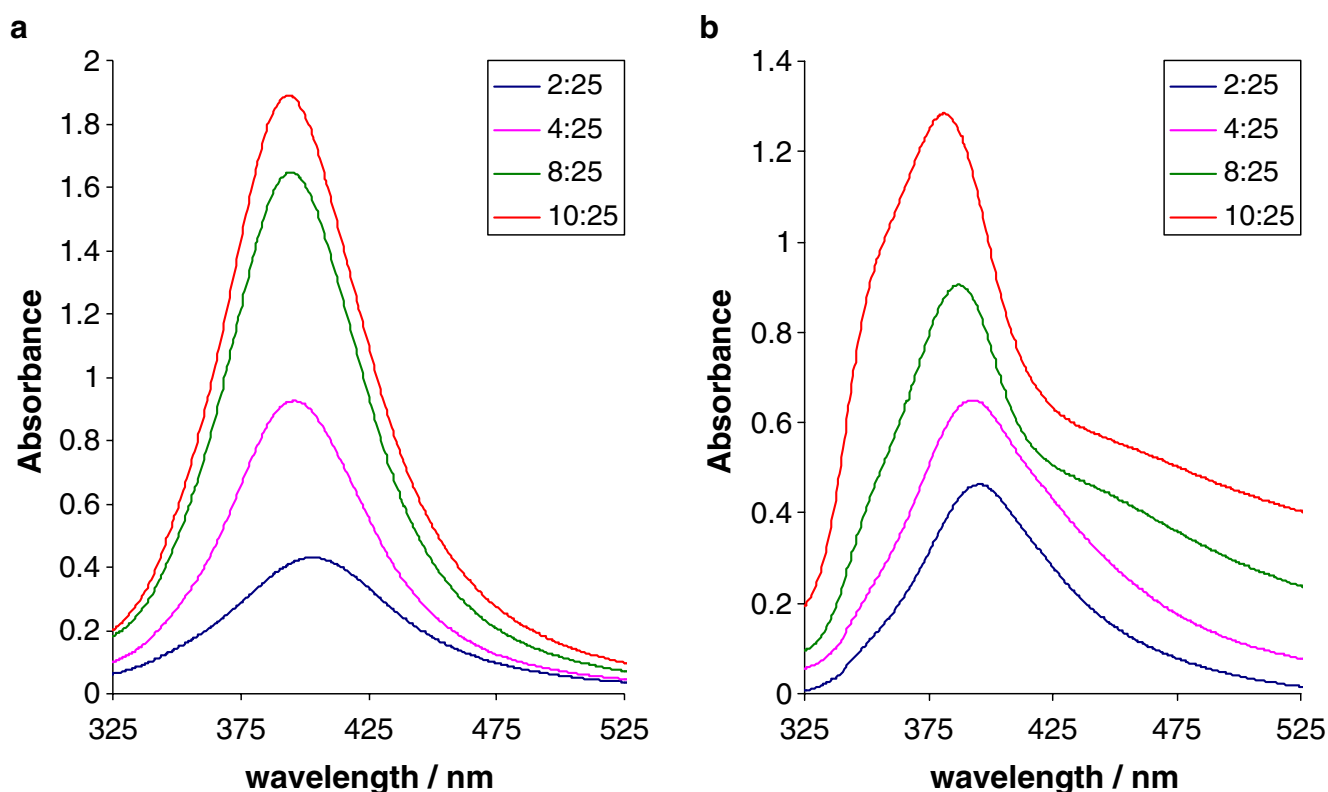
Fig. 2 a Absorption spectra of silver nanoparticles prepared using magnetic stirrer (2:25; volume ratio of aqueous solution of silver nitrate and sodium borohydride). **b** Absorption spectra of silver

nanoparticles prepared using ultrasonic field (2:25; volume ratio of aqueous solution of silver nitrate and sodium borohydride)

spherical objects with incident electromagnetic radiation. Electronic modes in silver nanoparticles are particularly sensitive to their shape and size, leading to pronounced effects in the visible part of the spectrum. The observed plasmon band shows that the silver nanoparticles are spherical in shape [30].

Quenching of fluorescence

Interaction with chemical species alters the electron density of the silver nanoparticles, thereby directly affecting the absorption of the surface bound organic moiety as well as surface plasmon absorption band. One can utilize these spectral shifts to measure the binding constants of fluorophores with silver nanoparticles. Dampening and broadening of the surface plasmon band was evident as these molecules complexed with the silver surface. In addition both the radiative and nonradiative rates depend critically on the size and shape of the nanoparticles, the distance between the dye and the nanoparticles the orientation of the molecular dipole with respect to the dye-nanoparticle axis and the overlap between the molecular emission with the nanoparticles absorption spectrum.

A fluorophore is an oscillating dipole. Nearby metal surfaces can respond to the oscillating dipole and modify

the rate of emission and the spatial distribution of the radiating energy. The electric field felt by a fluorophore is affected by interactions of the incident light with the nearby metal surface and also by interaction of the fluorophore oscillating dipole with the metal surface. Additionally, the fluorophore oscillating dipole induces a field in the metal. These interactions can increase and decrease the field incident on the fluorophore and increase and decrease the radiative decay rate [31].

To investigate the size effect of metal nanoparticles on the DHDMAQ absorption and emission profile, different sizes of silver nanoparticles were elegantly employed. Figure 3a, b and c show the absorption spectrum of DHDMAQ in methanol and absorption spectra of DHDMAQ in different sizes of silver nanoparticles respectively. Figure 4a, b and c depict the fluorescence emission spectrum of DHDMAQ in methanol and the fluorescence emission spectra of DHDMAQ in different sizes of silver nanoparticles respectively. The observed fluorescence quantum yield of DHDMAQ in different sizes of nanoparticles has been reported in Table 1. C.D. Geddes et al. described the effects of metallic silver nanoparticles and colloids on nearby fluorophores [32, 33]. Excited state fluorophores behaves as oscillating dipoles, which interact with free electrons in metals. These interactions can increase the radiative decay
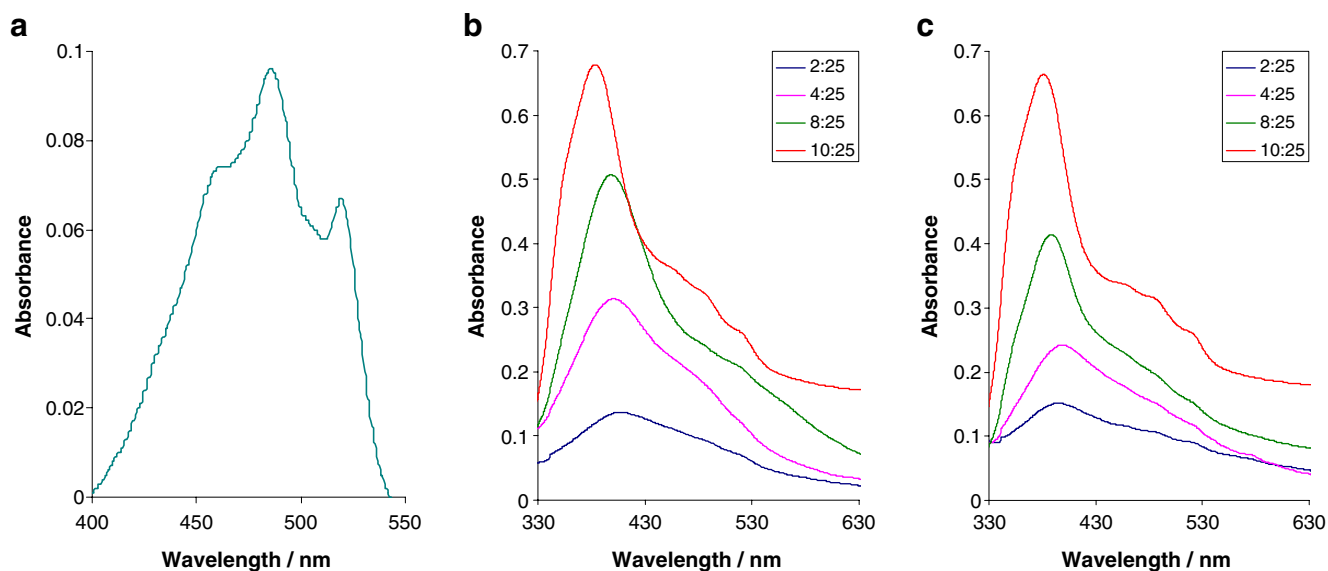
Fig. 3 **a** Absorption spectrum of DHDMAQ in methanol (concentration of DHDMAQ in methanol is 0.02 mM). **b** Absorption spectra of DHDMAQ in silver nanoparticles prepared using magnetic stirrer. **c** Absorption spectra of DHDMAQ in silver nanoparticles prepared using ultrasonic field

rate of fluorophores resulting in many desirable effects such as, increased quantum yields and decreased life times. But in the present case as the particle size decreases the fluorescence quantum yield value decreases. It may be due to the following reason.

It is well known that metallic surface induce strong quenching of molecular fluorescence due to electromagnetic coupling between the metal and the fluorescence molecule. Weitz et al. [34] proposed a model to afford a satisfactory treatment of nanoparticles-induced fluorescence quenching. The excitation of the electronic plasma resonance leads to an increase in the absorption rate. Again, the molecular emission dipole excites the plasma resonance leading to an increase in the rate of radiative decay. However, the non-radiative branch of the decay provides an additional damping effect, when the latter process overwhelms the other two processes, quenching of fluorescence is observed.

In the present case the excitation wavelength is 488 nm which does not coincide with the plasmon resonance peak of silver colloid and the silver nanoparticles do not exhibit any fluorescence. Therefore the change in the DHDMAQ absorption mediated by the electrical near field due to silver plasmon resonance is weak.
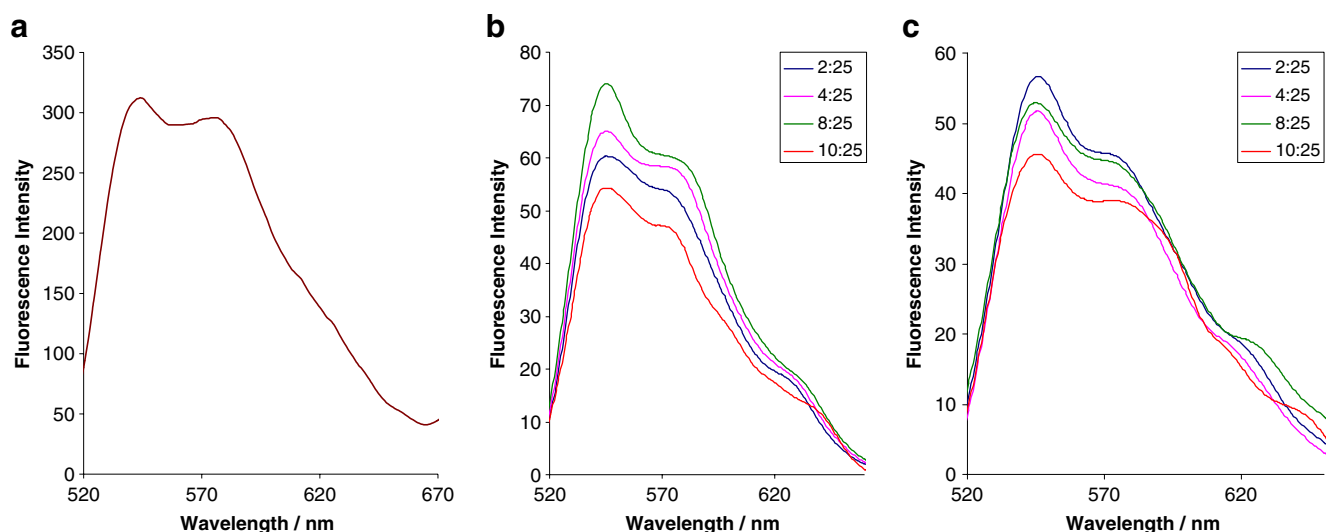

Fig. 4 **a** Fluorescence spectrum of DHDMAQ in methanol. **b** Fluorescence spectra of DHDMAQ in silver nanoparticles prepared using magnetic stirrer. **c** Fluorescence spectra DHDMAQ in silver nanoparticles prepared using ultrasonic field

The surface plasmon band of silver sol shows a maximum in the range 380–400 nm for different sizes of sol. When DHDMAQ is added to the silver sol, the plasmon band of silver shifts towards higher wavelengths and its intensity decreases. i.e. a damping of the plasmon band is observed (Fig. 3a, b and c). The damping of the silver plasmon band indicates the attachment of the DHDMAQ molecules on the particle surface.

Ditlbacher et al. [35] attempted to explain these peculiarities of molecular fluorescence near a metal surface. When using fluorescing molecules as local probes of the surface plasmon field of metallic nanoparticles, in the vicinity of a metal, the fluorescence rate of the molecules is a function of the distance between the probe molecule and the metal surface and when in direct contact with the metal, the fluorescence of molecules is completely quenched.

The distance of closest approach of the probe molecules to the nanoparticles core will change with the particle size. Thus the origin of the nanoparticles size dependence on the quenching process also lies in the core-size related difference in the density spectrum of the electronic states of the silver nanoparticles. Due to the chemisorption of the DHDMAQ to the silver surface, the molecular orbitals of the DHDMAQ molecules are mixed with the metallic band states. Certain orbitals of DHDMAQ interact strongly with the silver particles and are responsible for the chemisorption band, while others are little affected by adsorption [36]. Thus, the energy transfer quenching is also very sensitive to density of electronic state changes.

For dye-nanoparticle distances of 1 nm a static model should be accurate enough, hence an electrodynamical treatment is not necessary. With the Gersten–Nitzan model [37] the radiative rate is derived by assuming dipole emitters. Here the dipole for the entire system is considered, taking into account the intrinsic molecular dipole, the molecular dipole induced by the dipole field of the nanoparticles, the dipole of the nanoparticles driven by the dipole field of the adjacent nanoparticles and the dipole of the nanoparticles driven by the dipole field of the molecule. The resonant energy transfer of the molecular excitation is treated by calculating the absorption of the molecular dipole field at the position of the metal nanoparticles. The observed drastically decreased emission rate (lower quantum yield) is a consequence of a phase shift between the molecular and the metal dipole leading to a destructive interference effect.

It is well established that the binding of the probe molecules to the metal surface results in quenching of the excited states. Both electron transfer and energy transfer processes are considered to be the major deactivation pathways for excited fluorophores on the metal surface. The electron transfer mechanism is predominant for particle sizes of <5 nm as the particles do not exhibit any surface

plasmon band in the visible region [38, 39]. As the metal particles are larger than 5 nm, energy transfer dominates the quenching mechanism.

The degree of quenching depends on the structural details that control proximity between the fluorophore and metal nanoparticles core. When a donor molecule is placed in the vicinity of the conductive metal surface, resonant energy transfer between the donor and acceptor takes place [39]. The probability of this Forster energy transfer depends on the overlap of the emission band of the probe molecules with the absorption spectrum of the nanoparticles. In the present case there is no overlap of the emission band of DHDMAQ and the absorption spectrum of the silver nanoparticles which leads to the absence of Forster energy transfer between DHDMAQ and silver nanoparticles.

The surface plasmon efficiently acts as energy acceptor even at a distance of 1 nm between the probe molecules and the metal surface [40]. Metal nanoparticles also have a continuum of electronic states and exhibit energy transfer behavior as excited state quenchers [36]. The observed changes in absorbance of the absorption spectrum and fluorescence intensity reflects the alteration of the electronic properties of the DHDMAQ chromophore as it binds to the silver nanoparticles which act as a excited state quencher. The DHDMAQ has a high emission quantum yield in the absence of nanoparticles, the dominant effect for the quenching of excited state of DHDMAQ in silver nanoparticles may be due to radiative energy transfer to the metal surface. Fluorescence quenching may also result from a photo induced electron transfer process between the excited DHDMAQ and the silver nanoparticles. The interaction with the dye and excited state surface reactions may lead to morphological changes of the silver nanoparticles.

The Stern–Volmer equation accounting for both static and dynamic quenching is generally written as $\varphi_o/\varphi = 1 + K_{sv}$ [Ag] [31] where $K_{sv}=K_s+K_D$ where K_s and K_D are
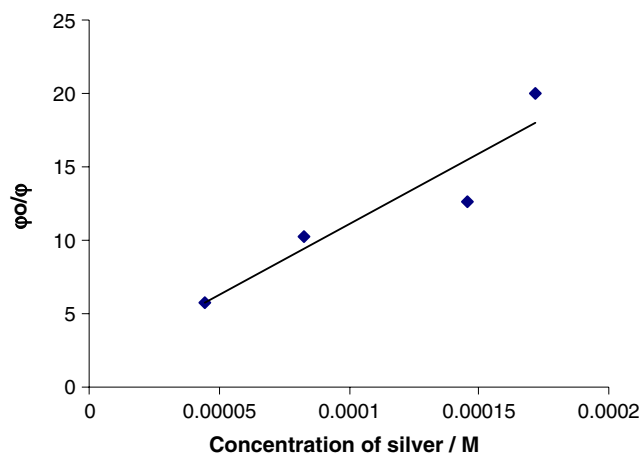
Fig. 5 Variation of φ_o/φ vs silver concentration (magnetic stirrer)

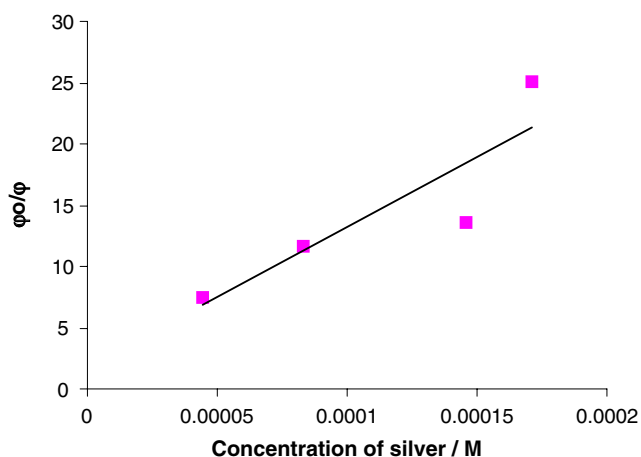**Fig. 6** Variation of φ_o/φ vs silver concentration (ultrasonic field)

the static and dynamic quenching constants respectively, φ_o and ϕ are the fluorescence quantum yield of DHDMAQ in the absence and presence of quencher [Ag], respectively. There is no possibility of formation of static quenching complexes via attractive electrostatic interaction between fluorophore–quencher pairs collisional quenching is effectively possible. Figures 5 and 6 show the plot of φ_o/φ vs silver concentration at constant DHDMAQ concentration. The plot is linear with $K_{sv} = 9.66 \times 10^4 M^{-1}$ and $11.48 \times 10^4\ M^{-1}$ in silver nanoparticles prepared by magnetic stirrer and ultrasonic field respectively. The linearity of the Stern–Volmer plot indicates that only one type of quenching occurs in the system. In the presence of quencher the absorption spectrum of DHDMAQ remains unaltered in frequency. This indicates that static quenching does not occur. The absence a new broad band indicates that
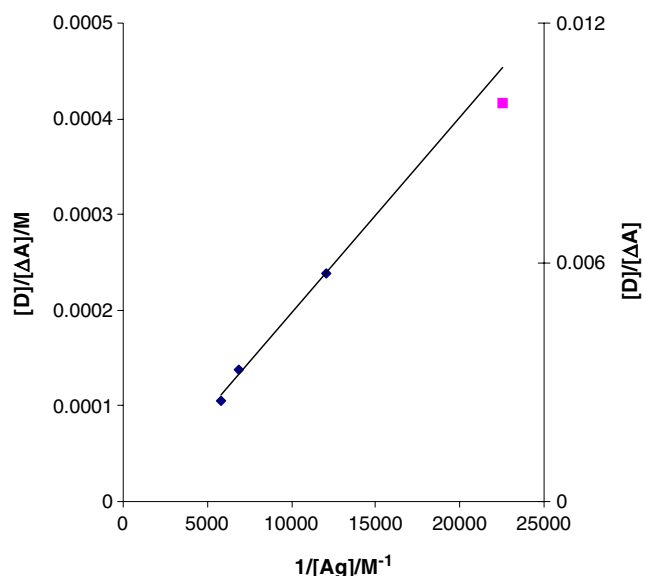
DHDMAQ has been bound to silver nanoparticles and so has failed to exhibit excimer and exciplex formation due to intermolecular interactions or if there is the formation of any trace of the excimer, it is also quenched by the metal. The Stern–Volmer quenching constant by silver nanoparticles in the solution is very high indicating the presence of adsorption of the dye molecule on the quencher surface. The high quenching efficiency of the solution results from the larger surface area provided by the smaller nanoparticles, which enhances their dye adsorption capability.

The association constant for the complexation between silver nanoparticles and DHDMAQ were obtained by analyzing the absorption changes (Benesi–Hildebrand approach). The association constant of $K_{ass}=450\ M^{-1}$ and $5555\ M^{-1}$ in silver nanoparticles prepared by magnetic stirrer and ultrasonic field respectively, was obtained from the plot of $[D]/\Delta A$ vs $1/[Ag]$ (Figs. 7 and 8) where $[D]$ is the concentration of DHDMAQ, ΔA is the changes in absorbance of DHDMAQ with and without silver nanoparticles and [Ag] is the concentration of silver. The high value of K_{ass} observed in these experiments suggests a strong association between the silver colloid and DHDMAQ.

The size regime dependence of the silver nanoparticles on the fluorescence quenching process can be rationalized by the correlation of the structures of the nanoparticles in terms of size. Having the same fluorescent probe and nanoparticle of different sizes we can realize the role of size and surface effect on the quenching. The smaller the particle, the larger is the surface area to volume ratio of
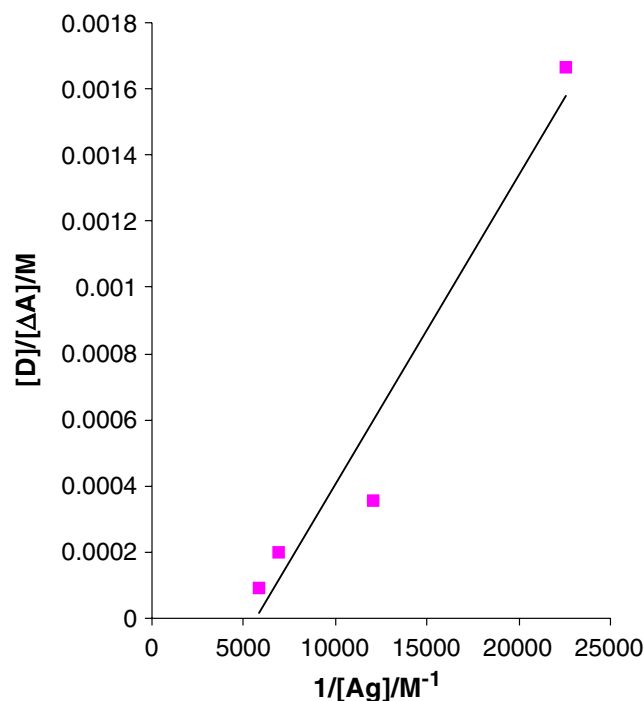

Fig. 7 Variation of $[D]/[\Delta A]$ vs $1/[Ag]$ for DHDMAQ in silver nanoparticles prepared by magnetic stirrer (pink color data not included)

Fig. 8 Variation of $[D]/[\Delta A]$ vs $1/[Ag]$ for DHDMAQ in silver nanoparticles prepared by ultrasonic field

the particles. The DHDMAQ molecules added to the nanoparticles are in thermodynamical equilibrium between the surface and aqueous phase and the only fluorescent component is the free DHDMAQ in the solution. The fluorescence is due to the unbound probe molecules in the system. The adsorption of the probe molecules from solution on to the nanoparticles surface is a function of the chemical composition and structure of the metal particles, as well as nature of the solution. For a fixed set of solution parameters, the adsorption process is only influenced by the particle size. As the size of the particles decreases, there is the increasing contribution of the surface atoms. The increased surface are with progressive decrease in particle size can accommodate large number of probe molecules around the silver particles. And therefore, smaller particles become efficient quenchers of molecular fluorescence than that of the larger ones. This result suggests that collisional quenching plays major role in the studied photo physical process in the presence of nano-particles.

Conclusion

Optical absorption and fluorescence emission techniques have been employed to study the photophysical properties of DHDMAQ on silver nanoparticles. The process of fluorescence quenching of DHDMAQ by silver nano-particles indicate that the collisional quenching occurs and the quenching depends on the particle size of the silver nanoparticles. The DHMAQ molecules were adsorbed on the surface of the silver nanoparticle which leads to quenching of fluorescence.

Reference

1. Mukherjee T (2000) Proc Indian Natl Sci Acad A 66:239
2. Butter J, Hoey BM (1987) Biochim Biophys Acta 925:144
3. Thomson RH (1971) Naturally occurring quinones. Academic, New York
4. Brigger I, Dubernet C, Couvreur P (2002) Adv Drug Deliv Rev 54:631
5. Joguet L, Sondi I, Matijevic E (2002) J Colloid Interface Sci 251:284
6. Tanaka T, Kohno H, Murakami M, Shimada R, Kagami S (2000) Oncol Rep 7:501
7. Eriksson M, Norden B, Eriksson S (1988) Biochemistry 27:8144
8. Nonaka Y, Tsuboi M, Nakamoto KJ (1990) J Raman Spectros 21:133
9. Feng ZM, Jiang JS, Wang YH, Zhang PC (2005) Chem Pharm Bull (Tokyo) 53:1330
10. Wang SX, Hua HM, Wu LJ, Li X, Zhu TR (1992) Yao Xue Xue Bao 27:743
11. Abo KA, Adeyemi AA, Sobowale AO (2001) Afr J Med Med Sci 30:9
12. Abo KA, Adeyemi AA (2002) Afr J Med Med Sci 31:171
13. Rosi NL, Mirkin CA (2005) Chem Rev 105:1547
14. Alivisatos P (2004) Nat Biotechnol 22:47
15. Kamat PV (2002) J Phys Chem B 106:7729
16. Merker M (1985) J Colloid Interface Sci 105:297
17. Pinna N, Weiss K, Sack-Kongehl H, Vogel W, Urban J, Pileni MP (2001) Langmuir 17:7982
18. Ivanisevic A, Mirkin CA (2001) J Am Chem Soc 123:7887
19. Imahori H, Norieda H, Yamada H, Nishimura Y, Yamazaki I, Sakata Y, Fukuzumi S (2001) J Am Chem Soc 123:100
20. Durbertret B, Calame M, Libchaber AJ (2001) Nat Biotechnol 19:365
21. Chatterjee S, Nandi S, Battacharya SC (2005) J Photochem Photobiol A Chem 173:221
22. Umadevi M, Vanelle P, Terme T, Rajkumar BJM, Ramakrishnan V, J Fluoresc doi:10.1007/s10895-008-0364-8
23. Creighton JA, Blatchford CG, Albrecht MG (1979) J Chem Soc Faraday Trans 2 75:790
24. Parker CA, Rees WT (1960) Analyst 85:587
25. Umadevi M, Vanelle P, Terme T, Ramakrishnan V (2006) J Fluoresc 16:569
26. Bohren CF, Huffman DF (1983) Absorption and scattering of light by small particles. Wiley, New York
27. Link S, El-Sayed MA (2003) Annu Rev Phys Chem 54:331
28. Valmalette JC, Lemaire L, Hornyak GL, Dutta J, Hofmann H (1996) Anal Mag 24:m23
29. Jingquan C, Suwei Y, Weiguo Z, Yi Z (2006) Front Chem China 4:418
30. Mock JJ, Barbic M, Smith DR, Schultz DA, Schultz S (2002) J Chem Phys 116:6755
31. Lackowicz JR (1999) Principle of fluorescence spectroscopy. Pleum, New York
32. Aslan K, Holley P, Geddes CD (2006) J Mater Chem 16:2846
33. Geddes CD, Cao H, Gryczynski I, Gryczynski Z, Fang J, Lakowicz JR (2003) J Phys Chem A107:3443
34. Weitz DA, Garoff S, Gersten JI, Nitzan A (1983) J Chem Phys 78:5324
35. Ditlbacher H, Krenn JR, Felidj N, Lamprecht B, Schider G, Salerno M, Leitner A, Aussenegg FR (2002) Appl Phys Lett 80:404
36. Huang T, Murray RW (2002) Langmuir 18:7077
37. Gersten J, Nitzan A (1981) J Chem Phys 75:1139
38. Ipe BI, Thomas KG, Barazzouk S, Hotchandani S, Kamat PV (2002) J Phys Chem 106:18
39. Fan C, Wang S, Hong JW, Bazan GC, Plaxco KW, Heeger AJ (2003) Appl Phys Sci 100:6297
40. Inacker O, Kuhn H (1974) Chem Phys Lett 27:317